

PROBABILISTIC SEISMIC ASSESSMENT OF A REGULAR STEEL MRF DESIGNED TO EUROCODE 8 PROVISIONS

A.K. Kazantzi¹, T.D. Righiniotis² and M.K. Chryssanthopoulos³

¹*Design Engineer, Tony Gee and Partners LLP, Esher, Surrey, UK*

²*Lecturer, University of Surrey, Faculty of Engineering & Physical Sciences, Guildford, Surrey, UK*

³*Professor, University of Surrey, Faculty of Engineering & Physical Sciences, Guildford, Surrey, UK*

Email: nkk@tgp.co.uk, t.righiniotis@surrey.ac.uk, mkchry@surrey.ac.uk

ABSTRACT :

The studies undertaken following the Northridge and Kobe earthquakes in 1994 and 1995, during which many steel buildings were hampered by unsatisfactory connection behaviour, also exposed limitations of the deterministic approaches in assessing the performance of new and existing buildings, thus leading to a renewed interest in probabilistic methods for earthquake engineering applications. The majority of the research has so far aimed at combining experimental and analytical efforts into seismic reliability methodologies for steel buildings typical of US practice. Corresponding studies on European steel Moment Resisting Frames (MRFs) are still to be developed and validated. Thus, the current study presents a probabilistic assessment carried out on a Eurocode 8-designed steel MRF, exploring explicitly the effect of joint ductility on its seismic reliability. Fragility curves are generated at different performance levels using the Monte Carlo simulation technique and performing time history analyses on the sample buildings subjected to a suite of ground motion records. Fragilities are presented for building realisations both with and without considering a limit in the total plastic rotational capacity of the beam-to-column joints. The rotational capacities are estimated using an empirical equation, derived from cyclic loading tests on European steel joints. A hazard study on a European site is combined with the structural fragility, thus evaluating the annual seismic risk. The results are used to quantify the notional reliability levels of a Eurocode 8-designed steel MRF.

KEYWORDS: Steel Moment Resisting Frames, reliability, fragility curves, joint ductility

1. INTRODUCTION

The unexpected connection damage sustained by many steel buildings during the Northridge and Kobe earthquakes in 1994 and 1995, posed questions on the efficiency of the hitherto adopted design and construction practices. In addition, the need to explore and quantify the risk induced by potentially unsatisfactory connection behaviour on the reliability of steel structures, stimulated major experimental and analytical studies in the USA, Japan and Europe. In the past few years these experimental and analytical efforts have been combined in fragility methodologies, which introduce uncertainty in both structural behaviour as well as ground motion characteristics. In its majority, this work has been focused on buildings typical of US practice (e.g. Luco and Cornell, 1998; Song and Ellingwood, 1999; Wang and Wen, 2000; Kinali and Ellingwood, 2007; Kazantzi *et al.*, 2008a). Similar fragility studies on European steel Moment Resisting Frames (MRFs) are lacking, even though it is generally recognised that design and construction practices are different compared to their North American counterparts.

In the present study, a fragility analysis is carried out on a regular EC8-designed, mid-rise building. Fragility curves are generated through inelastic time history analyses of randomly simulated building realisations subjected to an ensemble of European earthquake records and reported for three probabilistically defined performance levels. The probabilistic assessment explicitly accounts for the uncertainties related to the ground motion characteristics, the uncertainty in structural capacity due to the variability in material properties, as well as for the randomness in the global joint characteristics and the epistemic uncertainty associated with structural performance limits. Finally, the annual seismic risk is evaluated by convolving the mean fragilities with the seismic hazard scenario for the city of Reggio Calabria in Italy (Pinto, 2007).

2. BUILDING DESCRIPTION AND MODELLING

The regular, two-bay, five-storey frame considered here (see Fig. 1a) was designed by Fragiacommo *et al.* (2004), using the recommendations of EC3 (2005) and EC8 (2002). All beams and columns are assumed to be made of Fe360 (nominal yield stress 235MPa) European steel profiles. The frame was designed to be of high ductility class (implying a behaviour factor q of 6). The base shear was evaluated by means of EC8 design spectrum for soil type B combined with a design peak ground acceleration a_g of 0.35g. The elastic design spectral acceleration was evaluated to be approximately equal to 0.4g. The fundamental elastic period T_1 of the building was found to be 1.25sec.

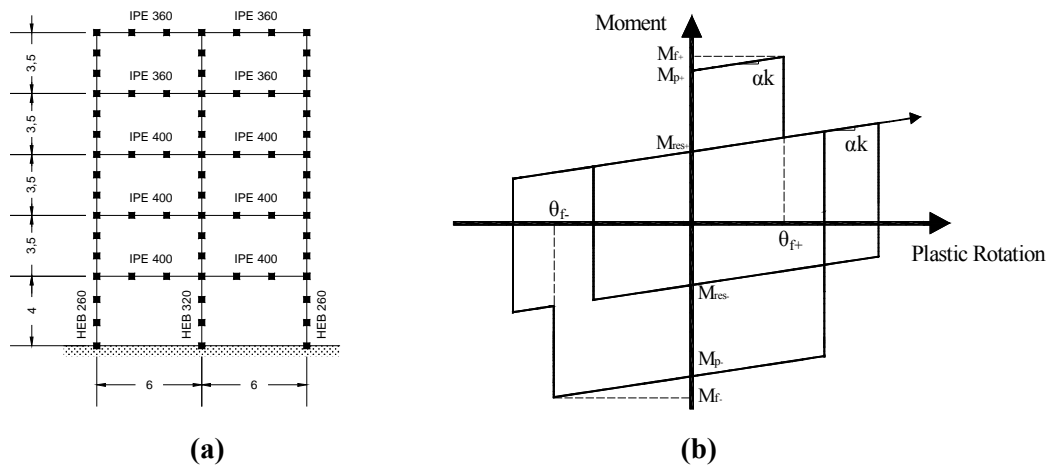


Figure 1 (a) Model of the EC8-designed steel MRF and (b) connection hysteresis model

Time history analyses of the frame shown in Fig. 1a were carried out using the computer program DRAIN-2DX (Prakash *et al.*, 1993). Rayleigh damping of 5% is assumed at the first two modes of vibration. At the plastic hinge location in beams and columns, a bilinear non-degrading hysteresis model with a constant 3% strain hardening is used. Shear deformations as well as the axial load-bending moment interaction (P-M) are accounted for according to the EC3 (2005) recommendations. In terms of the joint hysteretic behaviour, no distinction is made in this study between different failure modes. Thus, plastic behaviour and/or fracture is assumed to be captured through the same hysteresis loop. Accordingly, a special zero length failure element (Foutch and Shi, 1997) is introduced at the beam ends. The hysteretic behaviour of this inelastic spring is shown in Fig. 1b. The post-yield rotational stiffness of the spring is set equal to 3% of the elastic flexural stiffness k of the beam ($\alpha = 0.03$). As can be seen, failure is captured in both positive and negative bending. The ratio M_{res}/M_p is assigned an arbitrary value of 0.1.

3. PROBABILISTIC MODELLING

3.1. Failure rotation of joints

At performance levels associated with highly nonlinear structural responses, structural modelling of the rotational capacity of the joints needs to address potential failure modes. For the beam-to-column joints of the frame shown in Fig. 1a the positive (θ_{f+}) and negative (θ_{f-}) failure limits shown in Fig. 1b, which are assumed to be equal, are predicted by means of an empirical equation recently proposed by Kazantzi *et al.* (2008b). This equation was obtained by a regression analysis of the test data following a review on European experimental studies performed on rigid connections, which tend to display stable hysteretic characteristics. The reviewed database consisted of tests on fully welded connections, on connections bolted and welded on site and on bolted connections with extended end plates. Notwithstanding the differences between the specimens in terms of their

column section and applied column loading, connection typology (welded-bolted) and stiffener arrangement, the total (i.e. beam and panel zone) plastic rotation capacity of the joints was plotted against the beam depth, d (see Fig.2).

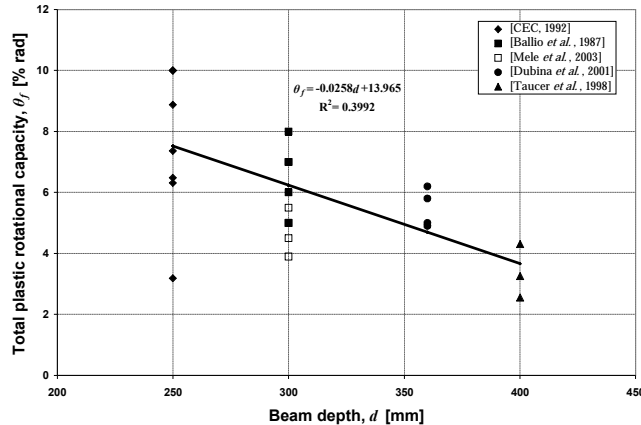


Figure 2 Total plastic rotational capacity (θ_f) vs beam depth (d)

A linear regression analysis of the test data yielded the following equation for the total plastic rotation capacity of the joint θ_f (% rad) with respect to the beam depth, d (mm):

$$\theta_f = -0.0258d + 13.965 . \quad (3.1)$$

Thus, in the following θ_f is assumed to be lognormally distributed with its mean value obtained using Eqn. 3.1 and a CoV of 30% (Kazantzi *et al.*, 2008b). In terms of the spatial variability of θ_f for any frame realisation, external joints at any given floor are assumed to be represented via identically distributed and fully correlated random variables. On the other hand, variables are assumed to be statistically independent from floor to floor. The same idealisation is adopted for the internal joints at any one floor. In total, this idealisation results in 10 random variables associated with the frame's joint rotation capacities.

3.2. Yield strength

Yield strength variability in beams and columns and, consequently, in the plastic moment capacity M_p , is accounted for by using four independent and identically distributed random variables, one for each section type shown in Fig. 1a. All yield strengths are assumed lognormally distributed, with a mean value of 280MPa (JCSS, 2001) and a CoV of 7% (JCSS, 2001).

3.3. Interstorey drift limits

In order to assess the structural damages, the performance levels defined in FEMA 356 (2000) are adopted. FEMA 356 (2000) specifies three performance levels, namely, the Immediate Occupancy (IO), the Life Safety (LS) and the Collapse Prevention (CP), and associates these with interstorey drift angle limits of 0.7%, 2.5% and 5%, respectively. In this study, these performance limits are assumed to be random and lognormally distributed. The distributions are assigned mean values equal to the values specified in FEMA 356 (2000) with a CoV of 10% based on engineering judgment.

4. SEISMIC INPUT

To account for the uncertainty in the seismic input an ensemble of recorded accelerograms pertaining to stiff

soil conditions was used. The records were selected from the European Strong Motion Database (Ambraseys *et al.*, 2002) and form part of the common seismic scenario used in the LessLoss Sub-Project 9 (Pinto, 2007) applications.

5. RELIABILITY FORMULATION

Seismic fragility $F_R(z)$ is a function that describes the probability of exceeding a specified deterministic or random performance level, conditioned on an intensity measure. Thus,

$$F_R(z) = P[G(\mathbf{X}) \leq 0 \mid IM = z] \quad (5.1)$$

where $G(\mathbf{X})$ is the limit state function in terms of the random variable vector \mathbf{X} and IM is the intensity measure, which is consistent with the specification of the seismic hazard. The intensity measure selected in this study is the spectral acceleration at the building's elastic fundamental period and at 5% damping, $S_a(T_1, 5\%)$. Since the response statistics are assessed through interstorey drifts, Eqn. 5.1 may be written as

$$F_R(z) = P\left\{DL_{PL} - \max_i \left[\max_t \left(\frac{|u_i(t)|}{h_i} \right) \right] \leq 0 \mid S_a = z \right\} \quad (5.2)$$

where $0 < t \leq t_d$, DL_{PL} is the drift angle limit at the performance level under consideration, t_d is the duration of the ground motion, i is the storey level, u_i is the interstorey drift of the i^{th} storey and h_i is the storey height. By setting

$$\theta_{max} = \max_i \left[\max_t \left(\frac{|u_i(t)|}{h_i} \right) \right] \quad (5.3)$$

Eqn. 5.2 may also be written in a more compact form as

$$F_R(z) = P\{\theta_{max} \geq DL_{PL} \mid S_a = z\}. \quad (5.4)$$

6. FRAGILITY ANALYSIS

6.1. Record-to-record variability

Fragility curves are presented here based on a series of nonlinear time history analyses, on 200 sample buildings, at different intensities of earthquake excitation. For these analyses, fully ductile beam-to-column joints were assumed ('unlimited ductility') for the steel MRF. The building realisations were generated through Monte Carlo simulation using the Latin Hypercube Sampling technique (Ayyub and McCuen, 1995).

Fig.3 shows *CP*-related fragility curves. Each curve is conditioned on a particular accelerogram, scaled upward in intervals of 0.1g in accordance with the structure's spectral acceleration $S_a(T_1, 5\%)$, and accounts for the variability in beam and column yield strength and modelling uncertainty in capacity interstorey drift limits. By analysing an ensemble of input motions it is possible to estimate a median curve, which is also shown in Fig.3. Clearly, the effect of record-to-record variability on fragility estimation is very significant. The presence of outliers (for example the curve furthestmost to the right in Fig.3) suggests that the median would be a more robust estimator than the mean, especially when relatively small ensembles are considered. Fig.4 depicts the fragility curves pertaining to *LS* performance level together with the associated median curve. It can be seen that the record-to-record variability becomes less pronounced compared to the variability observed in the *CP* limit state. On that basis it can be said that the effect of record-to-record variability increases with increasing

nonlinearity in the response. This observation is further supported when considering the *IO* performance level whose corresponding fragility curves are presented in Fig.5.

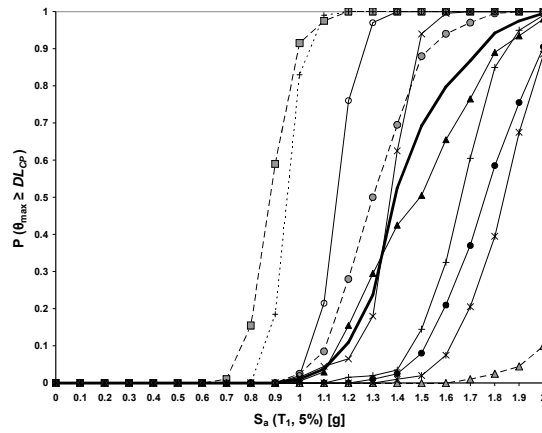


Figure 3 Fragility curves at the *CP* performance level ('unlimited ductility')

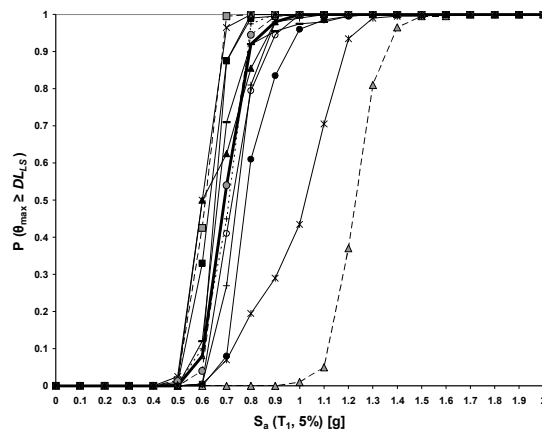


Figure 4 Fragility curves at the *LS* performance level ('unlimited ductility')

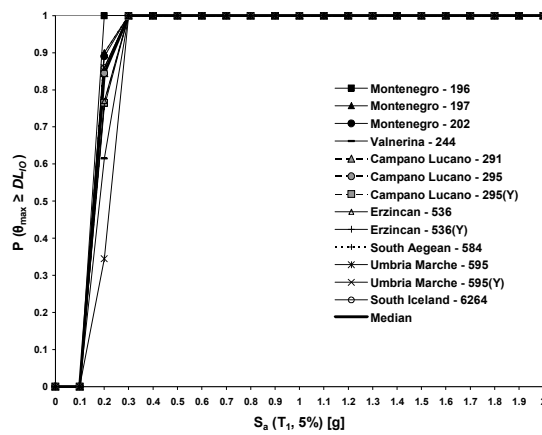


Figure 5 Fragility curves at the *IO* performance level ('unlimited ductility')

6.2. Effect of joint ductility

To investigate the effect of joint ductility and failure on the seismic fragility, the building's fragility curves are presented in this section considering potential joint failures. For these analyses, the 'finite ductility' hysteretic model was used (see Fig. 1b), which accounts for the existence of a finite θ_f .

In an identical manner to the fragility assessment presented in Section 6.1, fragility curves were obtained at the three examined performance levels (*CP*, *LS* and *IO*) considering though only nine ground motion records. Fig. 6 compares the mean fragility curves (average of nine curves) for the three limits states. For comparison purposes, mean fragility curves, obtained analysing the same MRF with fully ductile joints ('unlimited ductility') and considering the same nine recorded accelerograms, are presented in the same figure.

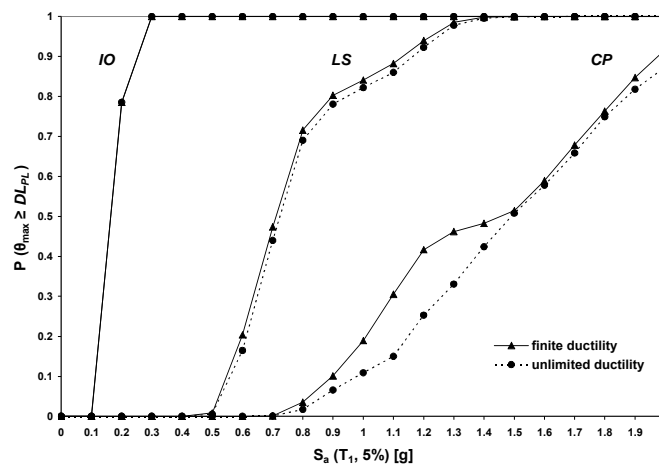


Figure 6 Mean fragility curves obtained for two levels of joint ductility

By comparing the mean fragility curves obtained using the 'finite ductility' and the 'unlimited ductility' constitutive models it can be seen that, the effect of joint failures is small at the *IO* and *LS* performance levels. By contrast, for the *CP* limit state their impact on the fragility is clearly noticeable. This observation was, more or less, expected, given that the local and global ductility capacities are interrelated. Thus, with mean joint rotational capacities ranging between 3.6%-4.7%, the MRF is anticipated to be able to sustain 0.7% and 2.5% drifts with no or limited joint failures, respectively. It is also worth mentioning that, for both cases considered, the estimated notional 'failure' probability at the building's elastic design spectral acceleration, the latter associated with an exceedance probability of 10% in 50 years, was estimated to be less than 5.6×10^{-4} for the *LS* performance objective.

7. SEISMIC HAZARD ANALYSIS

The mean fragility curves derived with respect to the different performance levels may be combined with the earthquake hazard to determine failure probabilities for any given structural system. The earthquake hazard accounts for the uncertainty associated with the ground motion at the specific site where the analysed structure is located.

The annual extreme seismic hazard that is used to perform the probabilistic hazard analysis is based on a study that was carried out for the city of Reggio Calabria in Italy (Pinto, 2007). The hazard curves presented in Fig. 7 pertain to periods which are close to the elastic fundamental period of the steel MRF. Also shown in Fig. 7 is the hazard curve at the building's fundamental period. This was obtained by interpolating between the curves

related to the 1 and 1.5sec periods.

Following the determination of the hazard curve, the building's annual failure probability at any particular performance level can also be estimated. The limit state probability or the probability of failure for a structure exposed to a single hazard can be expressed as (Ellingwood, 2001)

$$P_f = \int_0^{\infty} f_R(z)H(z)dz \quad (7.1)$$

where z is the chosen intensity measure, here being the spectral acceleration S_a , $f_R(z)$ is the probability density function of the fragility and $H(z)$ is the hazard function.

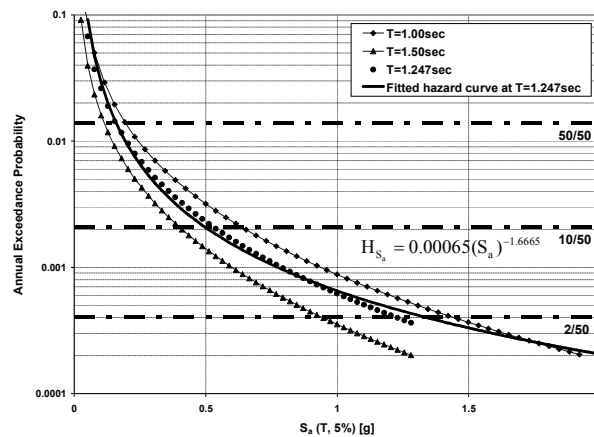


Figure 7 Annual extreme spectral acceleration hazard curves

Table 7.1 summarises the computed annual failure probabilities along with their associated reliability indices β . Results are shown in Table 7.1 for both the 'finite' and 'unlimited' ductility models. Hence, for example, the annual failure probability of exceeding the *LS* performance level was found to be 1.03×10^{-3} for the 'finite' and 9.94×10^{-4} for the 'unlimited ductility' model. In other words, it can be said that the *LS* limit state is on average exceeded once every 971 and 1006 years for the 'finite' and 'unlimited ductility' cases, respectively.

Table 7.1 Annual failure probabilities and reliability indices for the examined performance levels

	Annual Failure Probability (‘finite ductility’)	β	Annual Failure Probability (‘unlimited ductility’)	β
<i>CP</i>	3.97×10^{-4}	3.4	3.41×10^{-4}	3.4
<i>LS</i>	1.03×10^{-3}	3.1	9.94×10^{-4}	3.1
<i>IO</i>	8.51×10^{-3}	2.4	8.51×10^{-3}	2.4

8. CONCLUSIONS

This paper examined the seismic reliability of a steel MRF designed to EC8 provisions. Analytical fragility curves were obtained for a mid-rise regular steel frame at three performance levels and for two levels of joint ductility.

The study demonstrated the significant effect of the acceleration signature on the global uncertainty. It was also revealed that the effect of joint rotation capacity is clearly noticeable on the mean fragility corresponding to high seismic demand and response levels. By contrast, the effect of joint failures was found to be almost unnoticeable on the mean fragilities associated with low to moderate deformation demands. Finally, on the

basis of the evaluated annual failure probabilities, obtained using the results from an existing hazard study at a site in Italy, the notional reliability of the analysed EC8-designed steel MRF may be considered satisfactory, for the examined range of performance levels, provided that acceptable construction quality has been achieved.

REFERENCES

- Ambraseys, N., Smit, P., Sigbjornsson, R., Suhadolc, P. and Margaris, B. (2002). Internet-site for European strong-motion data, European Commission, Research-Directorate General, Environment and Climate Programme.
- Ayyub, BM. and McCuen, RH. (1995). Simulation-based reliability methods, In: Sundararajan, C., editor, Probabilistic structural mechanics handbook, Chapman and Hall, New York.
- Ellingwood, BR. Earthquake risk assessment of building structures. *Reliability Engineering and System Safety* **74:3**, 251–262.
- European Committee for Standardization. (2002). prEN1998-1: Eurocode 8: Design of structures for earthquake resistance—Part 1: General rules, seismic actions and rules for buildings, Brussels.
- European Committee for Standardization. (2005). EN1993-1-1: Eurocode 3: Design of steel structures—Part 1-1: General rules and rules for buildings, Brussels.
- FEMA 356. (2000). Prestandard and commentary for the seismic rehabilitation of buildings, Federal Emergency Management Agency, Washington, DC.
- Foutch, DA. and Shi, S. (1997). Connection element (type 10) for DRAIN-2DX, Internal Report, Department of Civil Engineering, University of Illinois at Urbana-Champaign, Urbana, IL.
- Fragiacomo, M., Amadio, C. and Macorini, L. (2004). Seismic response of steel frames under repeated earthquake ground motions. *Engineering Structures* **26:13**, 2021–2035.
- Joint Committee on Structural Safety (JCSS). (2001). Probabilistic model code Part 3: resistance variables, <http://www.jcss.ethz.ch>.
- Kazantzi, AK., Righiniotis, TD. and Chryssanthopoulos, MK. (2008a). Fragility and hazard analysis of a welded steel moment resisting frame. *Journal of Earthquake Engineering* **12:4**, 596–615.
- Kazantzi, AK., Righiniotis, TD. and Chryssanthopoulos, MK. (2008b). The effect of joint ductility on the seismic fragility of a regular moment resisting frame designed to EC8 provisions. *Journal of Constructional Steel Research* **64:9**, 987–996.
- Kinali, K. and Ellingwood, BR. (2007). Seismic fragility assessment of steel frames for consequence-based engineering: A case study for Memphis, TN. *Engineering Structures* **29:6**, 1115–1127.
- Luco, N. and Cornell, CA. (1998). Effects of random connection fractures on the demands and reliability for a 3-story pre-Northridge SMRF structure. Proceedings of 6th US national conference on earthquake engineering, Earthquake Engineering Research Institute, Seattle, WA.
- Pinto, PE., editor. (2007). Probabilistic methods for seismic assessment of existing structures, LessLoss Report No. 2007/06, IUSS Press, Pavia, Italy.
- Prakash, V., Powell, GH. and Campbell, S. (1993). DRAIN-2DX: Base program description and user guide, Report No. UCB/SEMM-93/17, Department of Civil Engineering, University of California, Berkeley, CA.
- Song, J. and Ellingwood, BR. (1999). Seismic reliability of special moment steel frames with welded connections: II. *Journal of Structural Engineering (ASCE)* **125:4**, 372–384.
- Wang, CH. and Wen, YK. (2000). Evaluation of pre-Northridge low-rise steel buildings. II: reliability. *Journal of Structural Engineering (ASCE)* **126:10**, 1169–1176.